PHYSICAL REVIEW A, VOLUME 61, 060705(R)

Charge-transfer dissociation of vibrationally cold HeH$^+$: Evidence for and lifetime of the $a\ ^3\Sigma^+$ metastable state

D. Strasser,[1] K. G. Bhushan,[1] H. B. Pedersen,[1] R. Wester,[2] O. Heber,[1] A. Lafosse,[3] M. L. Rappaport,[1] N. Altstein,[1] and D. Zajfman[1]

[1]*Department of Particle Physics, Weizmann Institute of Science, Rehovot, 76100, Israel*
[2]*Max-Planck-Institut für Kernphysik, D-69029 Heidelberg, Germany*
[3]*Laboratoire des Collisions Atomiques et Moléculaires (Unité Mixte de Recherche Université Paris-Sud et Centre National de la Recherche Scientifique, No. 8625), Bâtiment 351, Université Paris–Sud, F-91405 Orsay Cedex, France*

(Received 13 December 1999; published 16 May 2000)

Using an alternative technique to trap keV ion beams, the kinetic-energy release after dissociative charge transfer of vibrationally cold HeH$^+$ was measured. The results indicate that rapid radiative vibrational cooling takes place during the trapping, thus allowing a direct observation of the $a\ ^3\Sigma^+$ metastable state of HeH$^+$, which has been a subject of controversy in previous dissociative recombination experiments.

PACS number(s): 34.50.−s, 33.15.−e, 34.70.+e

The singly charged helium-hydride molecular ion HeH$^+$ is among the most elementary molecular ions. Having two electrons, it is isoelectronic with the hydrogen neutral molecule H$_2$, and as such it has been the subject of intense experimental and theoretical work [1–3]. An observable abundance of HeH$^+$ has been predicted to be present in regions of high ionization in interstellar space, in particular in stellar atmospheres and interstellar clouds [4]. So far, however, no evidence for infrared emission from HeH$^+$ has been found from these regions [5], whereas it has been observed in laboratory discharges for many years [6].

The first observation of the vibrational-rotational spectrum of the electronic ground state was performed by Tolliver *et al.* [7] using the Doppler-tuned ion-beam laser-spectroscopic technique. The dissociative recombination of HeH$^+$(HeH$^+ + e^- \rightarrow$ He + H) has generated enormous interest because of the unusual recombination process by which it occurs [8] and its impact on the calculated overall abundance of HeH$^+$ in interstellar space. The recombination cross section of HeH$^+$ was originally believed to be very low, and it came as a surprise when the measured cross section at low energy was found to be as large as 2×10^{-15} cm^2, using single-pass merged-beams techniques [9] and then heavy-ion storage ring techniques [10]. However, these results were challenged by a reexamination [11] of the data taken from the single-pass experiment. It was proposed that the large recombination cross section was due to the presence of the lowest metastable triplet excited state ($a\ ^3\Sigma^+$) in the beam of HeH$^+$. The production rate of this triplet state in an ion source was theoretically estimated [12], and it was suggested that the radiative decay of the HeH$^+$($b\ ^3\Sigma^+$) was responsible for the apparently large population of the $a\ ^3\Sigma^+$ state. On the other hand, using an imaging technique to measure the energy release in the dissociative recombination of HeH$^+$, it was experimentally proven [13] that the high cross section measured in storage rings originated from the lowest vibrational level of the ground electronic state ($X\ ^1\Sigma^+$).

There has never been any direct experimental observation of the metastable $a\ ^3\Sigma^+$ state. The only indication of a bound excited state was provided in a collision-induced dissociation experiment [14], although there has been no definite identification [15]. The lifetime is unknown, except for a rough estimate [11] where it was compared to the metastable state of He($2\,^3S$) with a lifetime of ~8000 s. The difficulty in observing the $a\ ^3\Sigma^+$ state comes from the poor overlap of its nuclear wave functions with the ground state of HeH$^+$: While the equilibrium distance for the $X\ ^1\Sigma^+$ state is 0.77 Å, the minimum of the $a\ ^3\Sigma^+$ state is calculated to be at 2.3 Å (see Fig. 1). The potential curve for the triplet state has been the subject of various theoretical calculations [3,16,17] and it is repulsive at small internuclear distances R, but is weakly attractive at large R due to polarization and exchange forces. For ^{4}HeH$^+$ the $a\ ^3\Sigma^+$ state has been calculated to support four vibrational states, the lowest one being bound by only 82 meV [11] (see inset in Fig. 1).

In the present work, we present an alternative technique for measuring the kinetic-energy release (KER) after charge-

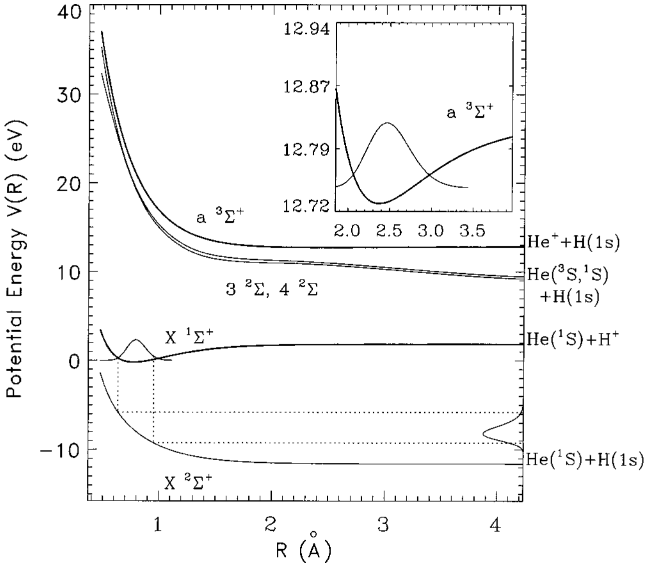

FIG. 1. Relevant potential curves for HeH$^+$ and HeH. The kinetic-energy release distribution expected for the ground state is schematically shown on the right-hand side. The inset shows an enlarged portion of the $a\ ^3\Sigma^+$ state.

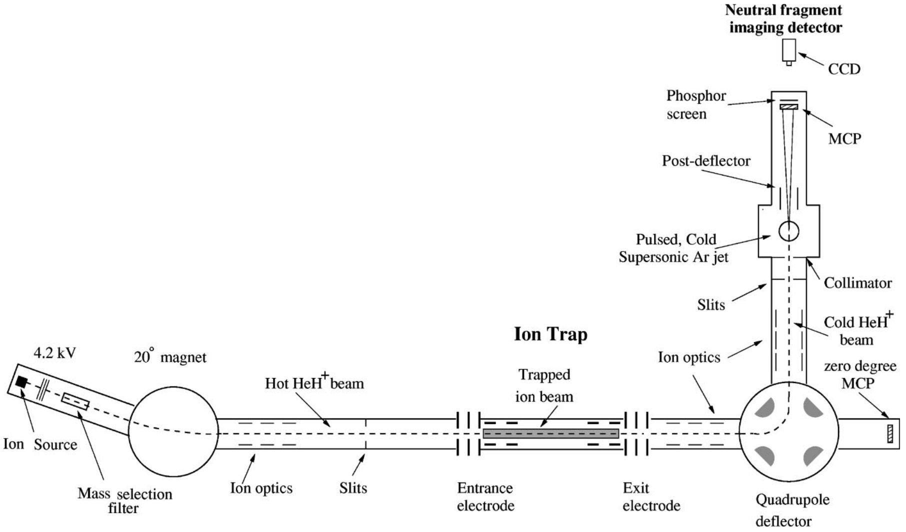

FIG. 2. Schematic view of the experimental setup. The vibrationally hot HeH^+ beam is produced in the ion source (left), stored inside the trap (center), and extracted toward the argon jet target where the CTD reaction occurs. The relative distance between the neutral fragments is measured using a three-dimensional imaging detector [23].

transfer dissociation (CTD) of vibrationally cold molecular ions. Using this technique we measure the KER of vibrationally cold HeH^+ molecules and directly observe the $a\,^3\Sigma^+$ metastable state. For HeH^+, the CTD process can be depicted as

$$HeH^+(v)+Ar \rightarrow He(n)+H(n')+Ar^+(E_k), \qquad (1)$$

where n and n' are the final quantum states of the He and H fragments, respectively. Figure 1 illustrates the dissociation mechanism for the known potential curves of HeH^+ and HeH. It can be seen that the KER reflects the initial internuclear distribution, which is given by the square of the vibrational wave function. The KER distribution $P(E_k)$ depends strongly on the initial vibrational population, which is usually a function of the ion source conditions and its mode of operation. Previous experiments for the CTD of HeH^+ were performed using molecular ion beams with undefined vibrational state populations [18,19].

The experimental setup is shown in Fig. 2. A 4.2-keV beam of HeH^+, produced from a mixture of 45% He, 45% H_2, and 10% Ar in an electron-impact ionization source, is trapped in an electrostatic ion trap [20,21]. The ion trap is made up of two sets of electrodes that act as electrostatic mirrors. During injection the voltage of the exit electrodes is switched on, while the entrance electrodes are switched off, so that the beam bounces back from the exit electrodes. When the trap is full, the entrance electrodes are rapidly (~ 100 ns) switched on. It has been demonstrated [20,21] that under certain focusing conditions of the mirrors, the trap is inherently stable, and beam loss occurs only because of collisions with the residual gas ($p \sim 10^{-10}$ Torr). About 10^5 ions are trapped at each injection. In the present experiment the trapping provides time for vibrational relaxation of the HeH^+ through radiative transitions between the various rovibrational levels. Equivalent storage, cooling, and extraction techniques for ion beams have been limited to large facilities, such as heavy-ion storage rings, using high-energy (MeV) beams [22].

Once stored, the beam can be extracted from the trap by lowering the voltages of the exit electrodes (see Fig. 2). The kinetic energy of the extracted beam is still 4.2 keV, except for a small fraction ($\sim 15\%$) that is located in the region of the exit mirror at the moment its voltages are switched off. This fraction is eliminated by deflecting the HeH^+ beam with an electrostatic quadrupole (see Fig. 2), which transmits only particles with the initial kinetic energy towards a pulsed supersonic jet of Ar atoms. The density of the target is low enough ($\sim 10^{12}$ atoms/cm^2) to insure single collision conditions, and the neutral particles produced by the charge-exchange process are detected downstream, while the remaining ions are steered away by an electrostatic deflector located a few centimeters after the interaction region. The KER of the two neutral fragments produced by the CTD process [see Eq. (1)] is determined using a three-dimensional imaging detector that measures both the position and the time of arrival of each fragment, one molecule at a time. Single neutral particles, which originate from the dissociation $HeH^+ + Ar \rightarrow He^+ + H + Ar$ (or $He + H^+$), are automatically discarded by this procedure. More details about the detector and its mode of operation can be found in Ref. [23].

The radiative lifetimes for the rovibrational levels in the ground electronic state of HeH^+ have been calculated by Datz and Larsson [24]. The slowest decay rate is for the $v=1 \rightarrow v=0$ transition and amounts to 2.5 ms for the rotational state $J=10$. Pure rotational transitions in the $v=0$ state are shorter than 5 ms for $J \geqslant 10$, but are longer than 100 ms for $J \leqslant 5$. At room temperature, only states below $J=4$ have a relative population larger than 5%, so it is expected that the beam is vibrationally cooled after a few tens of ms, but requires a much longer time to reach (rotational) equilibrium with the blackbody radiation of the trap at 300 K. Although it has been shown that the rotational temperature of HeH^+ produced in an electron-impact ion source is rather high ($T \sim 3100$ K) [25], the rapid transitions between the high rotational levels (lifetime ~ 0.5–3 ms) insure that no states above $J=10$ are significantly populated after 50 ms.

The KER distributions were measured for different storage times (0–200 ms). Figure 3 shows the distributions without storage [Fig. 3(a)] (i.e., the mirror electrodes grounded), for a storage time of 60 ms [Fig. 3(b)] and for a

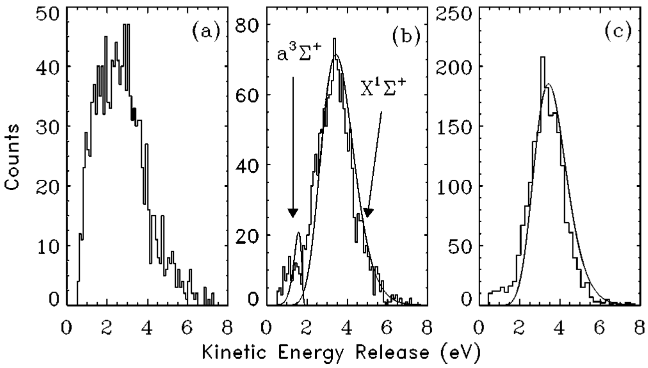

FIG. 3. Kinetic-energy release distribution for the charge-transfer dissociation of HeH^+ with Ar. Panel (a) is for a direct beam from the ion source, panel (b) is obtained after a storage time of 60 ms, while panel (c) is after 200 ms of storage time. The full line curves are KER distributions as calculated [Eq. (2)] for the ground state and for the $a\,^3\Sigma^+$ state. The calculations are normalized individually to the number of counts in each peak.

storage time of 200 ms [Fig. 3(c)]. As expected, the KER distribution after storage is narrower than the one without storage, demonstrating that rovibrational cooling takes place during storage. The spectrum for the vibrationally cold beam [Fig. 3(b)] can be compared to the expected distribution using the semiclassical projection method [26]. In this case, the KER distribution is given by

$$P(E_k)=P(R)\frac{dR}{dV}=|\Psi_0(R)|^2\frac{dR}{dV}, \tag{2}$$

where $\Psi_0(R)$ is the wave function for the ground vibrational state of HeH^+, and $V(R)$ is the dissociative $X\,^2\Sigma^+$ potential-energy curve of HeH (see Fig. 1). The full line shown in Figs. 3(b) and 3(c) shows the expected KER distribution based on Eq. (2), using the wave function calculated for the ground vibrational state of HeH^+ [27]. Although the overall agreement between the data and this simple model is good, there are two features that are significantly different.

First, the prediction of the model is shifted toward high energy $\Delta(E)$ compared to the measured distribution. Such a shift can be explained [26] qualitatively if one takes into account the dependence of the capture cross section on the energy defect, i.e., the difference between the ionization potential of HeH [$I_{HeH}=I_{HeH}(R)=7.5$ eV at 0.77 Å) and Ar$(I_{Ar}=15.75$ eV)]. A similar shift was observed by de Bruijn *et al.* [26] for CTD of H2+ with Ar, and it has been demonstrated that the capture cross section increases when the energy defect tends towards zero. In the present case, it is smaller at larger internuclear distance, and one expects an increase in the electron-capture probability for small KER, in agreement with the observation.

The second feature that is at odds with the calculated spectrum is the small peak located in the low KER part of the measured spectrum shown in Fig. 3(b), and to a smaller extent in Fig. 3(c). This small peak, which is centered at ~ 1.2 eV, is visible only after the vibrational cooling of the ground electronic state is completed. Previous experiments where the CTD of HeH^+ was measured (with a Cs target [18] or with a He target [19]) did not observe this peak as the beam was vibrationally hot, and hence the KER distribution produced by electron capture from the $X\,^1\Sigma^+$ state was too wide, as shown in Fig. 3(a). It must be pointed out that in [18], the peak at ~ 3 eV in the KER is assigned to radiative transitions from Rydberg states of HeH^+, and not to a direct capture to the ground state.

We have assigned the presence of the low KER peak seen in Fig. 3(b) to the electronic metastable state $a\,^3\Sigma^+$ of HeH^+(see Fig. 1). Such a state, when produced in the ion source, will most likely produce a small KER after CTD, as the minimum in the potential well is located at a large internuclear distance $(R\sim 2.2\,\text{Å})$. A simple projection of the square of the vibrational ground-state wave function of the $a\,^3\Sigma^+$ state on the ground dissociative state of HeH $(X^2\Sigma^+)$ would lead to a kinetic-energy release ($\sim 50-70$ meV) which is much smaller than the one shown in Fig. 3(b). The distance (and time) between the two fragments for this small KER is below the resolution of the present apparatus (the detection scheme did not allow us to measure events with an energy release of less than 0.5 eV). However, Orel, Kulander, and Rescigno [28] have recently calculated potential-energy curves of neutral doubly excited repulsive states that converge to the ionic $a\,^3\Sigma^+$ and $A\,^1\Sigma^+$ states, and thus lie below the metastable state of interest. Among the seven states, two $^2\Sigma$ states (see Fig. 1) have slopes which are large enough to lead to a measurable KER after CTD. Using Eq. (2) and the squared wave function for the vibrational ground state of the $a\,^3\Sigma^+$ state, we obtain a KER distribution that peaks at ~ 1.5 eV. The calculated distribution is shown in Fig. 3(b) as a full line, and is in reasonable agreement with the measured distribution, considering the fact that the exact slopes of the dissociative neutral states are not well known at the internuclear distance of interest (2.2 Å).

The main problem of this interpretation is the large energy defect resulting from the electron capture in the $^2\Sigma$ doubly excited states. These states lie only ~ 2 eV below the $a\,^3\Sigma^+$ state, and cannot be accessed by near-resonant charge transfer. This is also the reason why the predissociation of the $A\,^2\Sigma^+$ state of HeH is not seen in the present experiment, while it was clearly observed in collision with Cs atoms [18]. On the other hand, it has been demonstrated that for large energy defects, other processes such as electron promotion are dominant [26]. For example, in a previous measurement of CTD of H_2^+ at keV energies [29], it was shown that the transition to the predissociative $c^3\Pi_a$ state of H_2 was stronger for a He target than for an Ar target, although the process was far off resonance, and the energy defect was increased by almost 10 eV when changing the target from Ar to He $(I_{He}=24.6\,\text{eV})$. Moreover, because of the large internuclear distance of the $a\,^3\Sigma^+$ bound state, we expect the capture cross section to be much larger than for a similar transition from the ground state of HeH^+. As pointed out above, the main transition is probably to the dissociative ground state of HeH, but the small KER resulting from such a transition cannot be measured with the present setup. Thus, the exact relative population of the metastable state in the beam is difficult to estimate as it cannot be directly extracted from the data shown in Fig. 3.

It is clearly seen that the contribution of the metastable state to the KER distribution in Fig. 3(c) is smaller that in Fig. 3(b), by a factor of 2, demonstrating that this feature is definitively due to the presence of a metastable state. A more complete measurement of the lifetime of the $a\,^3\Sigma^+$ using the present extraction technique is quite difficult because of the low duty cycle of the experiment, but a rough estimation based on the data shown in Figs. 3(b) and 3(c) would lead to a value in the range of a few hundreds of milliseconds, a value that is much shorter than the lifetime of $\mathrm{He}(2\,^3S)$.

We hope that the present observation of the metastable $a\,^3\Sigma^+$ state of HeH^+ will stimulate additional theoretical calculations, especially related to its lifetime. In this work, we have also demonstrated an alternative method for trapping, storing, and extracting ion beams of keV energies. Application of this method to the cooling of molecular ions has been illustrated, but we believe that the advantageous configuration of this setup will open new and exciting possibilities in other fields, and it is expected that new types of experiments will be suggested and carried out in the near future.

This work has been funded by the German Federal Minister of Education, Science, Research and Technology (BMBF) within the framework of the German-Israeli Project Cooperation in Future-Oriented Topics (DIP).

---

[1] G. Glockler and D.L. Fuller, J. Chem. Phys. **1**, 886 (1933).

[2] D.M. Bishop and L.M. Cheung, J. Mol. Spectrosc. **75**, 462 (1979).

[3] T.A. Green, H.H. Michels, and J.C. Browne, J. Chem. Phys. **69**, 101 (1978), and references therein.

[4] W. Roberge and A. Dalgarno, Astrophys. J. **255**, 489 (1982).

[5] J.M. Moorhead *et al.*, Astrophys. J. **326**, 899 (1988).

[6] T.R. Hogness and E.C. Lunn, Phys. Rev. **26**, 44 (1925).

[7] D.E. Tolliver, G.A. Kyrala, and W.H. Wing, Phys. Rev. Lett. **43**, 1719 (1979).

[8] S.L. Guberman, Phys. Rev. A **49**, R4277 (1994).

[9] F.B. Yousif and J.B.A. Mitchell, Phys. Rev. A **40**, 4318 (1989).

[10] C. Strömholm *et al.*, Phys. Rev. A **54**, 3086 (1996), and references therein.

[11] F.B. Yousif *et al.*, Phys. Rev. A **49**, 4610 (1994).

[12] M.I. Chibisov, F.B. Yousif, P.J.T. Van der Donk, and J.B.A. Mitchell, Phys. Rev. A **54**, 4997 (1996).

[13] J. Semaniak *et al.*, Phys. Rev. A **54**, R4617 (1996).

[14] J. Schopman and J. Los, Physica (Utrecht) **51**, 132 (1971).

[15] K.R. Dastidar and T.K. Dastidar, J. Phys. B **9**, 1163 (1976).

[16] H.H. Michels, J. Chem. Phys. **44**, 3834 (1966).

[17] W. Kolos, Int. J. Quantum Chem. **10**, 217 (1976).

[18] W.J. van der Zande, W. Koot, and D.P. de Bruijn, Phys. Rev. Lett. **57**, 1219 (1986).

[19] W. Wu, M.H. Prior, and H. Bräuning, Phys. Rev. A **57**, R5 (1998).

[20] D. Zajfman *et al.*, Phys. Rev. A **55**, R1577 (1997).

[21] M. Dahan *et al.*, Rev. Sci. Instrum. **69**, 76 (1998).

[22] Z. Amitay *et al.*, Science **281**, 75 (1998).

[23] Z. Amitay and D. Zajfman, Rev. Sci. Instrum. **68**, 1 (1997).

[24] S. Datz and M. Larsson, Phys. Scr. **46**, 343 (1992).

[25] J.-C. Houver *et al.*, Int. J. Mass Spectrom. Ion Phys. **4**, 137 (1970).

[26] D.P. de Bruijn, J. Neuteboom, V. Sidis, and J. Los, Chem. Phys. **85**, 215 (1984).

[27] T.A. Green *et al.*, J. Chem. Phys. **61**, 5186 (1974).

[28] A.E. Orel, K.C. Kulander, and T.N. Rescigno, Phys. Rev. Lett. **74**, 4807 (1995).

[29] M. Vogler, Z. Phys. A **288**, 7 (1978).